National Renewable Energy Laboratory
Innovation for Our Energy Future

A national laboratory of the U.S. Department of Energy
Office of Energy Efficiency & Renewable Energy

Measurement of Depositing and Bombarding Species Involved in the Plasma Production of Amorphous Silicon and Silicon/Germanium Solar Cells

Annual Technical Report
1 June 2002 — 31 May 2005

A. Gallagher, K. Rozsa, P. Horvath, and D. Kujundcik
National Institute of Standards and Technology
Boulder, Colorado

Subcontract Report
NREL/SR-520-40056
June 2006

NREL is operated by Midwest Research Institute • Battelle Contract No. DE-AC36-99-GO10337

Measurment of Depositing and Bombarding Species Involved in the Plasma Production of Amorphous Silicon and Silicon/Germanium Solar Cells

Annual Technical Report
1 June 2002 — 31 May 2005

A. Gallagher, K. Rozsa, P. Horvath, and
D. Kujundcik
National Institute of Standards and Technology
Boulder, Colorado

NREL Technical Monitor: B. von Roedern

Prepared under DOE/GO Interagency Agreement No. DE-AC36-02GO10244

Subcontract Report
NREL/SR-520-40056
June 2006

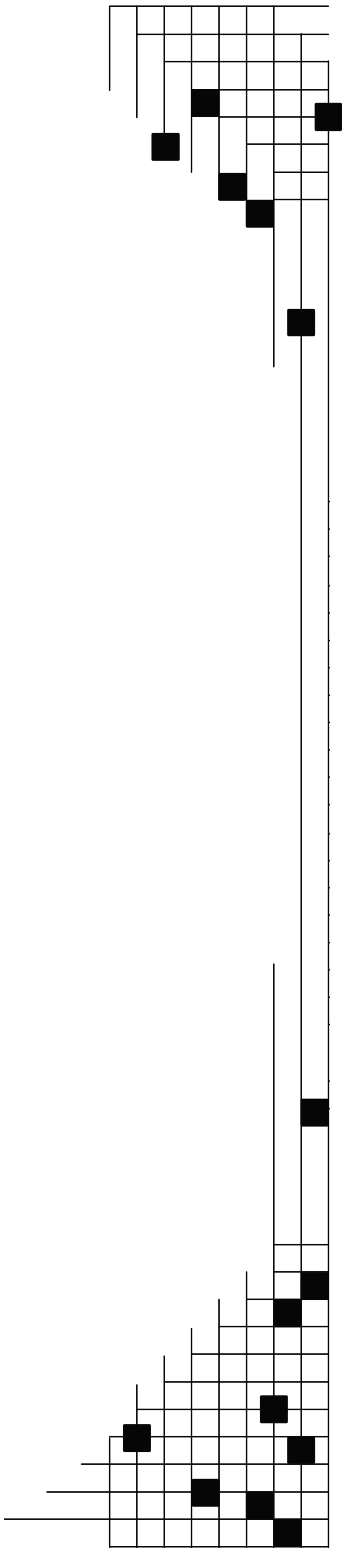

National Renewable Energy Laboratory
1617 Cole Boulevard, Golden, Colorado 80401-3393
303-275-3000 • www.nrel.gov

Operated for the U.S. Department of Energy
Office of Energy Efficiency and Renewable Energy
by Midwest Research Institute • Battelle

Contract No. DE-AC36-99-GO10337

NOTICE

Available electronically at http://www.osti.gov/bridge

Available for a processing fee to U.S. Department of Energy
and its contractors, in paper, from:

U.S. Department of Energy
Office of Scientific and Technical Information
P.O. Box 62
Oak Ridge, TN 37831-0062
phone: 865.576.8401
fax: 865.576.5728
email: mailto:reports@adonis.osti.gov

Available for sale to the public, in paper, from:

U.S. Department of Commerce
National Technical Information Service
5285 Port Royal Road
Springfield, VA 22161
phone: 800.553.6847
fax: 703.605.6900
email: orders@ntis.fedworld.gov
online ordering: http://www.ntis.gov/ordering.htm

This publication received minimal editorial review at NREL

Printed on paper containing at least 50% wastepaper, including 20% postconsumer waste

Table of Contents

List of Figures

Abstract

The properties of an apparatus designed to measure silane and silane/hydrogen discharge radicals by threshold ionization mass spectroscopy are described. We report measurements of these radicals, as well as discharge ions, at the substrate of an RF (13.6 MHz) discharge in pure silane and hydrogen/silane mixtures with (inlet flow) density ratios R = 16 and 36. The discharge gap, pressure, temperature and power are adjusted to fit typical amorphous or microcrystalline silicon device-production conditions. Amorphous silicon film deposition rates are measured, to relate the discharge conditions to those used in device-production reactors. Radical and ions densities at the substrate have been measured for the molecular species Si_xH_n with x = 0,1,2. The primary depositing radicals in the pure-silane discharge are SiH_3 and Si_2H_2, while the other SiH_n and Si_2H_n become significant in the hydrogen-diluted discharges. Discharge ions are dominated by Si- containing ions ($Si_xH_y^+$), even in highly hydrogen diluted vapors. However the heavier ions (x > 1) are more important as the silane fraction increases, and the H content (y value) is lower in pure silane.

Objective

The objective of this study is to measure the molecular species that lead to the growth of hydrogenated amorphous silicon (a-Si:H) and microcrystalline silicon (μc-Si) photovoltaic (PV) devices from RF discharges. Neutral radicals produce most of the film growth during this PV-device production, and by implication radicals primarily determine the device structure and electrical characteristics. The most important feature of the present experiment is thus the measurement of neutral-radical fluxes to the substrate. Additional depositing species that can influence film properties are positive ions and silicon-based particles produced by the discharge; we also measure these positive-ion species here. Some studies have already measured some of these radical and positive-ion species in silane and silane/argon discharges, but not for discharge conditions similar to those used to produce most photovoltaic devices. Our objective is to measure all of these species for conditions typically used for device production. In particular, we have studied 13.6 MHz-excited discharges in pure silane and silane/hydrogen vapors.

Introduction

The reactor is a small-scale version of an industrial PV-production reactor, utilizing similar electrode gap, temperature, gas pressure, gas mixtures and discharge power density. Gas flow is adjusted to produce similar dwell times to industrial reactors, or shorter times to clarify the influence of gas depletion and modification by the discharge. The reactor contains pure silane or mixed silane and hydrogen, under conditions typically used to produce hydrogenated amorphous (a-Si:H) and microcrystalline (μc-Si) silicon solar cells. Radio frequency (RF) discharges are studied, as these are most commonly used for industrial production of solar cells. Our primary interest is in measuring radicals that produce the devices in RF discharge, H_2/SiH_4 mixtures, as these are most frequently used for device production. However, to improve understanding of the deposition

chemistry, it is also useful to compare the radicals from various H_2/SiH_4 mixtures to those from a pure silane vapor. We utilize threshold ionization mass spectroscopy (TIMS) to detect the radicals that pass through a small orifice in the substrate. None of these radical fluxes to the substrate have previously been measured for the pressure range and deposition-rate conditions typically used for device production. However, quite a few measurements have been made in low pressure, high power density discharges, as described next.

Some of the first discharge-radical measurements in silane discharges were done at this laboratory, using TIMS.[1,2] These observations demonstrated important radical chemistry and the dominance of SiH_3 deposition for conditions used to produce good quality a-Si:H films. However, they used a DC discharge at low (< 0.1 Torr) silane pressure, with varying Ar dilution. Thus, they did not provide radical data for hydrogen dilution or for RF discharges, as is now used for device production. For the last 20 years the laboratory of Toshio Goto has used optical methods to detect the radicals Si, SiH, SiH_2 and SiH_3. These observations have yielded valuable radical-silane reaction rate constants, and confirmed the importance of SiH_3.[3,4,5] However, they have been carried out only in low pressure gases with very high power loading, yielding a mixture of radicals that is expected to be very different than under the high pressure, low power conditions normally used to produce photovoltaics. (Microcrystalline Si can be produced with some discharges studied.) Moreover, most of the measurements utilize a DC hollow cathode or ECR discharge. Jerome Perrin and collaborators have also studied radicals in RF silane discharges for many years, using TIMS.[6,7] They have measured the very important surface reaction probabilities of several radicals on a-Si:H and uc-Si. However, most of their measurements utilize very low silane pressure (0.06 Torr) and high power density, hence the observed radical densities do not apply to device production conditions. The exception is a 1 Torr, SiH_4/H_2 = 1/1 discharge[6] that produced 1.2 nm/s film growth; conditions that cause major particle growth. This yielded large SiH_3 and Si_2H_5 densities, with most of film growth produced by the SiH_3. In contrast to these prior studies, the present research utilizes 0.3 Torr pure silane or 1.5 Torr SiH_4/H_2 mixtures with ratios (1/R) of 1/20 and 1/40. The film growth rate, which characterizes the discharge power density, is also normally a low (~0.1 nm/s) value, as used to produce the best a-Si:H films.

This project has been staffed by three scientists, in addition to the PI, Alan Gallagher. Dr. Karoly Rozsa, a senior scientist from Budapest, Hungary, with many years of discharge experience initiated the design and construction phases. After about a year he was joined by two graduate students: Peter Horvath, a Physics Department student of Budapest University, and Damir Kujundzic, a EE student at the University of Colorado. Dr. Rozsa had other responsiblities at his Budapest laboratory, and left about halfway through the program. Damir Kujundzic also left about two years into the program, and essentially all measurements were carried out by Peter Horvath. He is currently analyzing these results and incorporating them into his thesis at Budapest University. We will publish them after his graduation and our analysis is completed. The data presented in this report is thus somewhat preliminary, and may be corrected or further analyzed in the publications.

Apparatus

1. Overview

The reactor is a small-scale version of an industrial PV-production reactor, utilizing a similar electrode gap (2 cm), temperature (~100 °C), gas pressures (0.3-2 Torr), gas mixtures and discharge power density. The latter is typically adjusted to produce 0.1-0.3 nm/s film growth rates, again as is commonly produced in industrial reactors. But in contrast with industrial reactors, this experimental reactor is about 8cm diameter and will normally be isothermal. Gas flow is adjusted to produce similar dwell times to industrial reactors, or shorter times to clarify the influence of gas depletion and modification by the discharge. The reactor contains pure silane or mixed silane and hydrogen, under conditions typically used to produce hydrogenated amorphous (a-Si:H) and microcrystalline (μc-Si) silicon solar cells. Radio frequency (RF) discharges are studied, as these are most commonly used for industrial production of solar cells.

As mentioned in the Introduction, the neutral radicals have been measured using threshold ionization mass spectrometry (TIMS). In this technique, an electron beam of near-threshold energy ionizes the radicals, and the ions are collected by a quadrupole mass spectrometer (QMS). This discriminates against the same ions produced by fragmentation of stable gases, since the threshold energy for the dissociative process is higher than for radical ionization without dissociation, usually by a few eV. As an example, the threshold for producing SiH_3^+ from the SiH_3 radical is 8.1 eV, and from SiH_4 is 12.3 eV. To confirm that the radical is actually being observed in the presence of much higher densities of parent gases, ions are collected while the electron energy is scanned through the threshold energy region.

This project required developing a new experiment, requiring apparatus design, construction and testing before data could be obtained. However, the TIMS method had previously been used in this laboratory and other laboratories. The TIMS method can detect very small radical fractions within their parent molecular gas, as is needed for diagnosis of these discharges. However, the ionization efficiency is much smaller than in conventional mass spectrometry, and good electron-energy control and ion collection efficiency is required. Thus, a unique apparatus design, geared to this application, is necessary, and is shown diagrammatically in Fig.1. The quasi-neutral plasma (glowing) portion of the discharge is shown diagrammatically; other dimensions are only representative. Gas flows mostly over the top of the RF electrode and across it to a pumping orifice at the bottom. (The orifice size is adjusted to yield the desired gas flow.) A 0.4 or 1 mm diameter orifice (#1) in the grounded (substrate) electrode allows radicals and ions, accompanied by the discharge gases, to exit toward the QMS. Since the QMS and electron multiplier (EM) must operate at pressures below 10^{-5} Torr, while the discharge operates at 0.2-2 Torr, several stages of differential pumping are required to prevent most discharge gases exiting orifice #1 from reaching the QMS. The first stage is provided by Pump 1, which also handles the full gas load. The next stage, which is separated from the first by a 1 mm x 4 mm slot-aperture (#2), includes the ionizer region and is evacuated by pump 2. The final stage is separated from the ionizer region by a 2

mm diameter QMS entrance aperture (#3), and is evacuated by pump 3. Pump 1 is a 300 liter/s turbomolecular pump, while pumps 2 and 3 are 50 liter/s turbomolecular pumps. An electron multiplier after the QMS allows single-ion sensitivity.

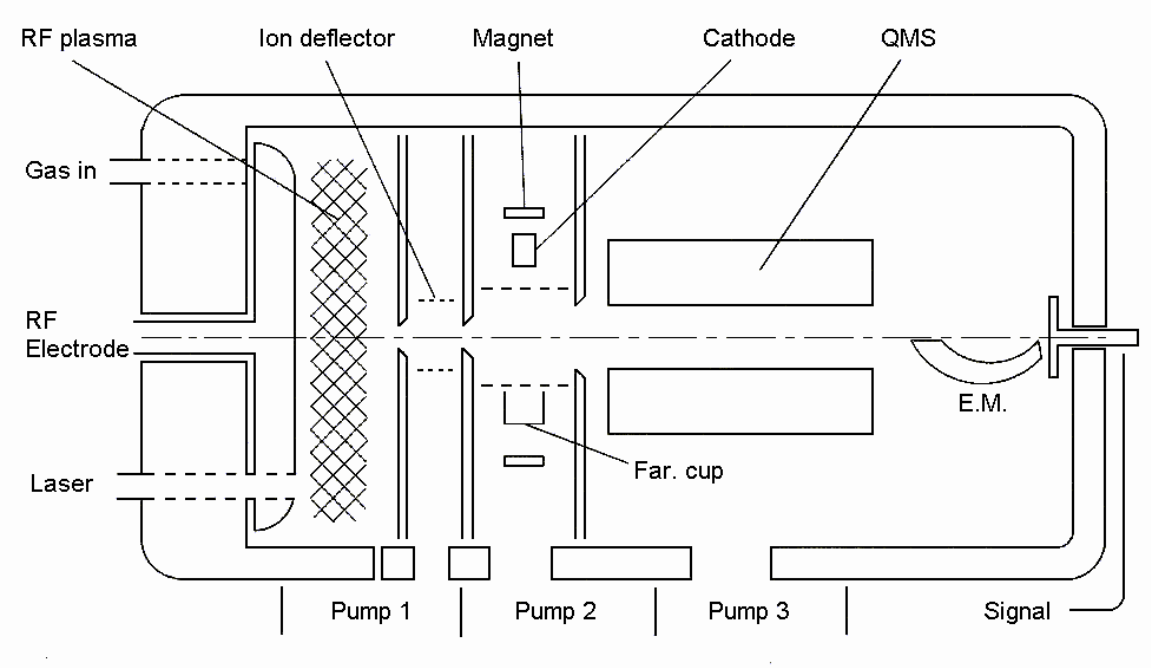

Fig.1. Diagrammatic representation of the apparatus designed for discharge radical detection by threshold ionization mass spectrometry. Discharge radicals pass through an aperture (#1, farthest left) into the ion deflector region, then through a slot (# 2, middle) into the ionizer region, which is evacuated by pump 2. Ions from this region are focused through an aperture (#3, farthest right) into the mass spectrometer, which is evacuated by pump 3. When biased, the ion-deflector screens prevent discharge ions from entering the mass spectrometer, for detecting neutral radicals, and discharge ions are studied by removing the bias.

Devices are normally deposited onto heated substrates, at temperature T_S, and this can influence discharge operation and chemistry. Thus, it is useful to study depositing species over a temperature range of 25-250 °C. While the RF electrode is not directly heated in most reactors, its temperature typically rises to 50-90 % of T_S. In our small, experimental reactor it is not practical to attempt reproducing this temperature gradient between the electrodes. We therefore heat the entire discharge region, and in the present design the entire apparatus, to the desired T_S.

An additional apparatus feature allows *in-situ* measurement of film growth rates. A laser beam that passes through a small orifice in the RF electrode (lower left in Fig.1) and is detected after reflecting off the growing film and substrate. This provides instantaneous film growth data, since the reflected intensity undergoes interference fringes that depend on film thickness. We and other researchers have frequently found that discharge optical

emission can provide a valuable diagnostic of silane-containing discharges. Thus, we utilize a discharge-viewing window to measure discharge emission.

We utilize full computer control of the experiment and data collection, using National Instruments input-output cards and LabView programming. We control the discharge power and timing and the QMS settings, and recording several types of data. The data includes the discharge pressure, RF voltage, ionizer electron beam current and energy, the a-Si:H film growth rate, and the ion signal from the mass spectrometer.

2. Electron Beam

A critical component of the apparatus is the ionizer, shown diagrammatically in the center of Fig.1. Here a magnetically-confined electron beam, of typically 1 μA, crosses the ionization region and is collected in a cup on the opposite side. The cathode is operated at the lowest possible temperature that will yield this current, since the high-energy thermal tail of the electron-energy distribution will produce an interfering ion signal from the parent gases. The ionization region is enclosed with a screen, to assure equipotential surfaces necessary for efficient ion collection, while allowing gases to be efficiently pumped away. The electron beam current is controlled by a "anode" immediately in front of the cathode, so that it can be held constant while the electron energy is scanned in TIMS. A "Faraday cup" collects this current for control and analysis.

The pressure in the ionizer region is considerably higher than in the QMS region. This is not expected to influence the electron or ion motion as long as pressures are too low to initiate a hot-cathode discharge, but silane reactions with the cathode surface can cause a loss of electron emission. The magnetic field (~ 40 Gauss) is sufficient to confine the electron beam, but too small to influence the ion motions. In addition, the location and size of the magnets is designed to minimize the fringing magnetic field in the RF plasma region. In practice, this fringing field will be a few Gauss, which minimally influences the discharge since $\nu_{Coll} >> \nu_{Cyl}$, where ν_{Coll} is the electron collision frequency and ν_{Cyl} the electron cyclotron frequency. The actual ionizer structure, and its mounting to the QMS, is shown in Fig.2.

Electron beam tests yielded the desired 1-5 μA current at 8-12 eV energy from "oxide" cathodes at 800-900 °C. This is quite satisfactory, particularly as tests in the presence of ~ 10^{-4} Torr silane yielded long operation at relatively stable 1 μA currents. The current passes through a 1 mm hole in an "anode" ~ 2 mm from the cathode emitting surface. The anode voltage is held constant relative to the cathode, providing a constant current while the electron energy (cathode voltage) is scanned. If a much larger current were used, the electrons would produce a "space charge depression" of the potential in the ionization region, while the accompanying electric fields distort ion motion and diminish ion collection efficiency. These fields are proportional to the electron current and relatively independent of the electron beam size, so it is necessary to limit the electron current in the indicated range. The ~ 1mm electron beam diameter provides a relatively compact ion source region for focusing into the QMS.

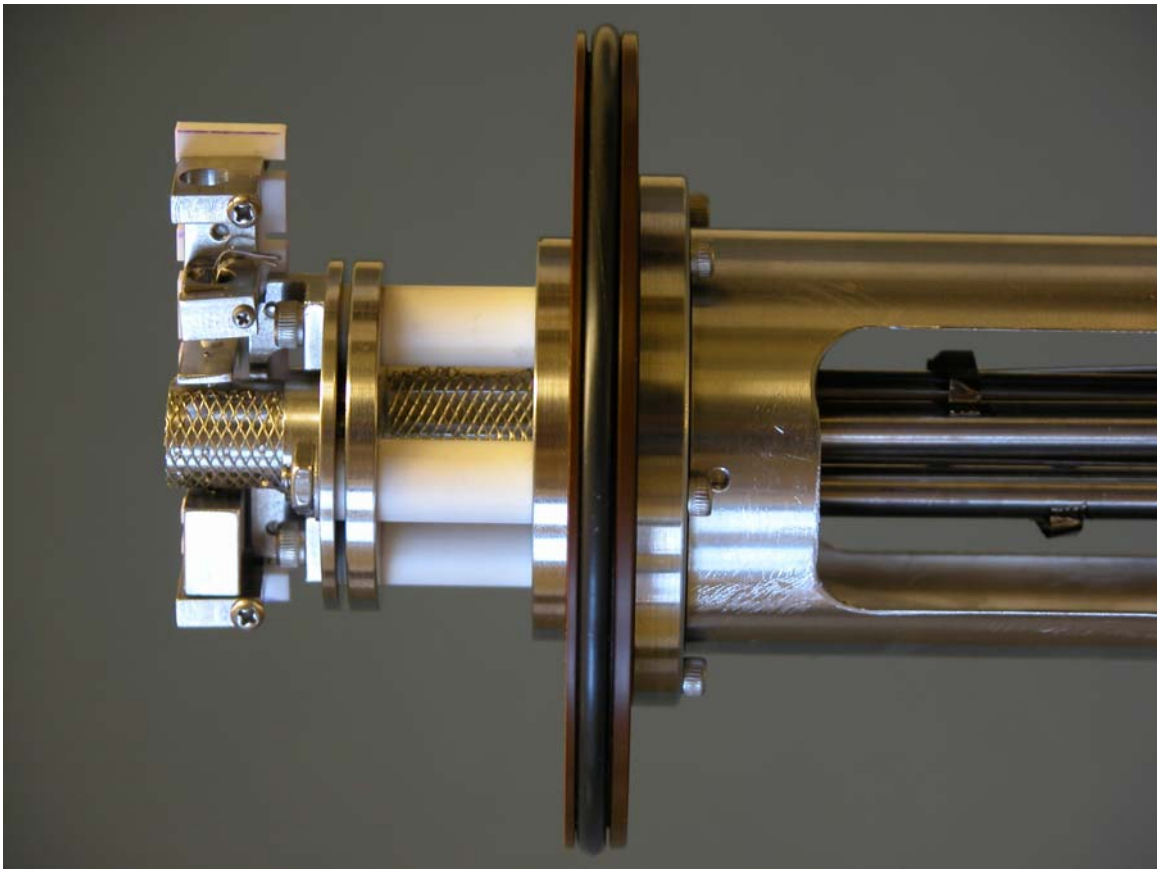

Fig.2. Photograph of the ionizer and ion optics mounted on the QMS. The rods of the QMS are visible at the right, inside the ~ 2" diameter supporting cylinder. The o-ring in the center of the figure is mounted on a polyimid disc that separates the ionizer and QMS regions.

3. Ion Collection

The ion collection efficiency is a crucial element of TIMS, since the small electron current and threshold-region ionization cross section yield much smaller ionization rates than in conventional mass spectrometry. Thus, in our design a coaxial screen applies a relatively strong electric field at the ionization location, to draw out essentially all ions and focus them into the QMS orifice. The typical bias of 30 V on this nearby "drawout" lens can also overcome fields due to surface potential variations. However, this also produces an electron energy spread in the ionization zone, so this field must not be too large.

Studies of the TIMS apparatus indicate that the ion collection efficiency of the ion-optics and QMS is typically one percent of total radical ionization. This is attributed primarily to a very small diameter of the QMS inlet that achieves ion transmission. This slows data collection but does not preclude the desired radical observations.

The electrostatic lenses that focus ions into the mass spectrometer are shown in more detail in Fig. 3, where calculated ion orbits are also shown. Due to necessity of detecting low radical densities at the substrate, and the small fraction of radicals exiting the substrate orifice that are ionized by the electron beam, it is important to have efficient ion collection into the MS. The radicals expand thermally from the substrate orifice, and when ionized the ions initially have almost the same (vector) velocity, as if they had started at the orifice. The ion optics is therefore designed to focus the substrate orifice into the MS input orifice. This design, and its performance, will now be presented.

An electrostatic lens is always positive, with a strength that depends on the ratio (R_E) of ion kinetic energy entering and exiting the lens. Here the initial kinetic energy is the thermal energy, typically ~ 0.04 eV, and the ions are accelerated to ~30 eV in the first lens, so R_E is very large for this lens, that is between the grounded-screen, "source" electrode and the "First Ion Lens" electrode. This large R_E has two important advantages. First, the lens has almost the same strength for $R_E = 1000$ as for $R_E = 50$ (ie. for large R_E), and as a result the large spread of initial thermal energies does not produce a large spread of ion orbits. The second advantage of this large "Ion2" voltage is that it produces a strong electric field at the ion-source location. As a result, stray electric fields due to surface contact-potential differences and electron-beam space charge do not seriously perturb the ion orbits. The disadvantages of the large first-lens R_E, and the resulting short focal length, is that the image ("Image1") of the substrate aperture occurs only slightly beyond the lens plane (the plane between the grounded screen and "Ion2"), and the ions have a large angular spread at the image. The MS would not transmit a very large fraction of these ions. To overcome this we introduced lens two, between elements "Ion2" and "Ion3", to produce "Image2" at the MS input. This re-imaging lowers the ion angular spread entering the MS, allowing for higher MS ion transmission. The ion energy inside the MS is typically 7 eV, and "Ion2" is typically set to ~3 Volts, so the second lens decelerates the ions from 30 to 3 eV, and there is a third, weak ($R_E = 2.3$) lens at the MS orifice.

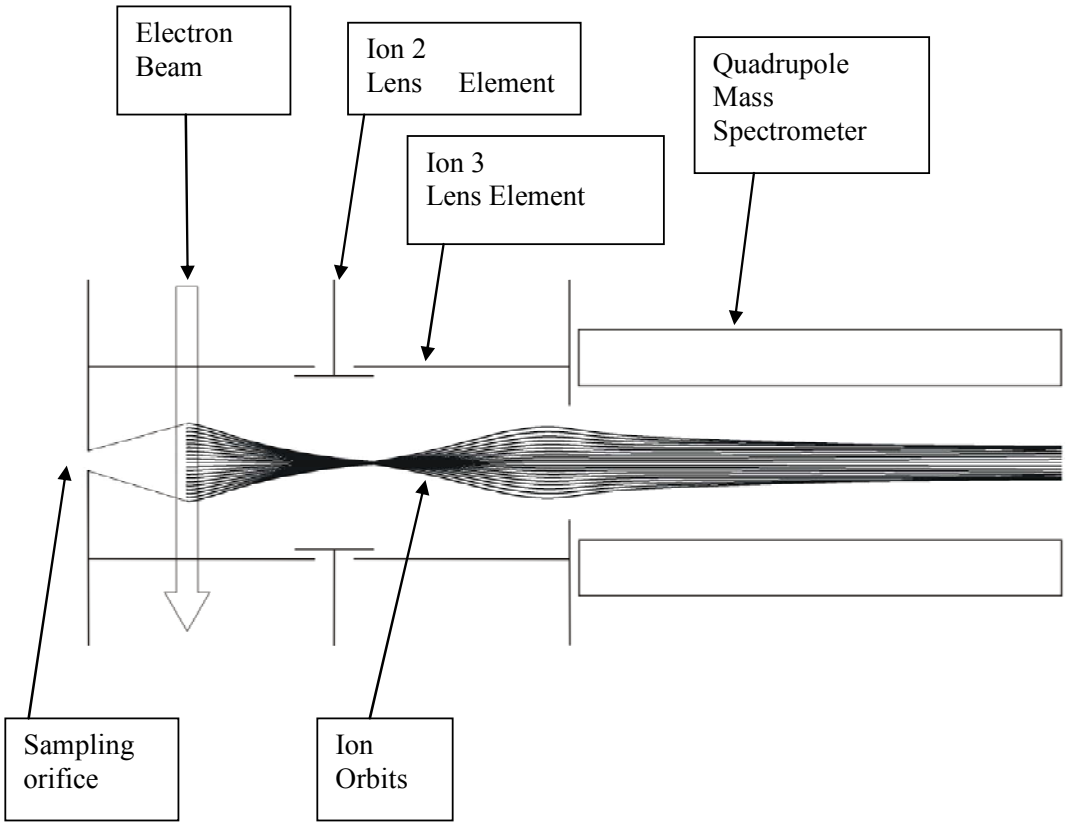

Fig.3. Diagram of the ion-collection region of the apparatus, and calculated ion orbits for V_{Ion2} = -30 V and V_{Ion3} = -2 V. The lens diameters are 1 cm, and the vertical dimension is expanded a factor of 3 (relative to horizontal) for clarity. The ionization occurs in a grounded-screen chamber, and the mass spectrometer is biased to -7 V.

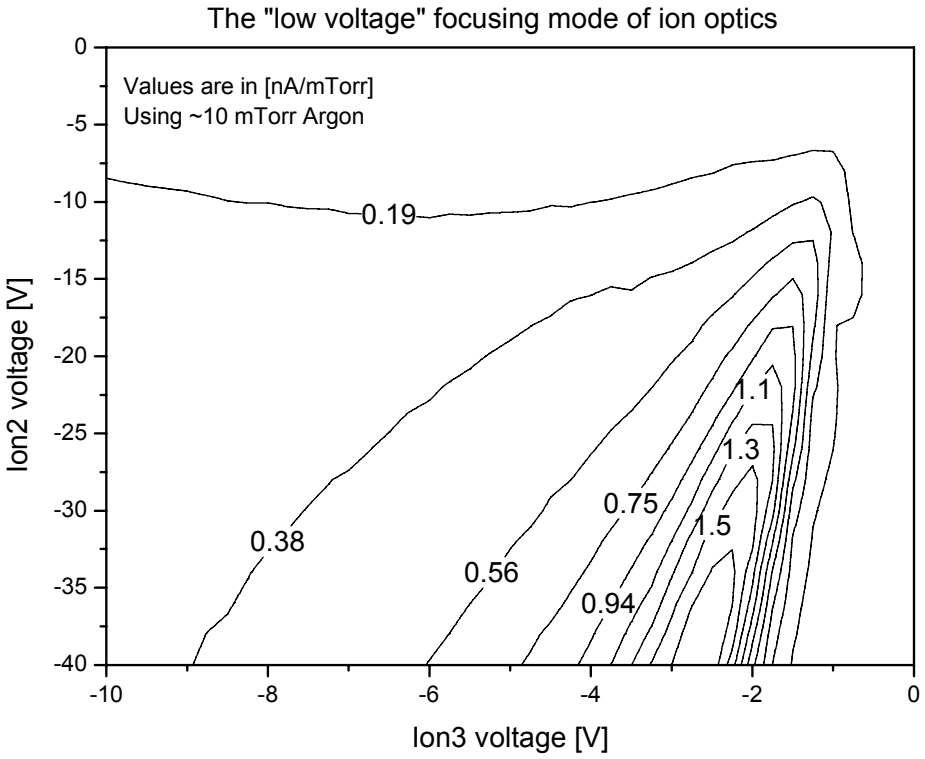

Fig.4. Dependence of the ion signals on ion-lens voltages.

The measured dependence of ion signal on the voltages of the ion-focussing lenses is shown in Fig.4. This compares favorably with ion-orbit calculation using the SIMION code, from which an example set is shown in Fig.3. By comparing the voltage dependencies of the SIMION orbits to the data in Fig.4, we conclude that the ion collection is working approximately as designed. It appears that ions from ~ 0.5 cm of electron-beam length, out of 1 cm inside the "source" screen region, are collected with good efficiency. To miminize contact potential differences, particularly in the presence of silicon deposition, the ion lens elements and the grounded screen are usually coated with "Aero Dag", a sprayed carbon black.

4. Discharge-Ion Background

The discharge-ion deflector shown in Fig.1 is a pair of screens biased to deflect discharge ions that exit through the sampling orifice. Several volts bias on one screen prevents most discharge ions from entering the QMS and interfering with the desired radical-ionization signals. This is a small enough voltage to prevent a discharge from developing in this region outside the main discharge. The flux of discharge ions at the substrate is typically only a few percent of the radical flux, but only ~ 10^{-7} of the radicals passing through the sampling orifice are ionized. Thus, the discharge-ions must be suppressed by a factor of

$>10^5$ to avoid a serious loss of signal/noise in the TIMS data. In practice, we have achieved suppression factors of 10^4-10^6 for the various ions and discharge conditions.

5. Quadrupole Mass Spectrometer

While some commercially available quadrupole mass spectromerters QMS can be adapted for TIMS measurements, they are quite expensive and the ionizer region would still have to be reconstructed and independently controlled. Thus, we have chosen to utilize and modify a QMS left over from another project in our laboratory. This includes replacing an unreliable "channel-plate" electron multiplier with a "Channeltron" electron multiplier from Burle Corp. This provides large and stable gain, allowing individual ions to be easily and reliably detected.

We utilize a Dycor/Amatec QMS for the radical detection, with the ionizer and ion collection portions modified for use in TIMS. We found the QMS electronics very unreliable, obscure and ill suited for our need to average weak ion signals during ionizing electron energy (E_{el}) scans under computer control. Thus, we have produced our own QMS electronics. This requires generating a fixed RF frequency and precisely controlling its amplitude (A) on the QMS rods, since A determines the transmitted mass. The DC rod voltages (V_{DC}) must reach hundreds of Volts (RMS) and be independently controlled, as this determines the transmission and mass resolution. The correlated A and V_{DC} are scanned under computer control to scan mass, or fixed during an E_{el} scan. A simple, inexpensive set of home-built electronics now provides these voltages under computer control, and QMS operation using this electronics is reliable and accurate. We have also provided for switching the QMS RF frequency between 2 and 5 MHz, where the former is best for the mass range corresponding the $Si_xH_n^+$ peaks with x = 1-3, and the latter allows H_n^+ (n = 1-3) ions to be collected without major interference from the "zero-mass" peak. The final mass spectrometer development was to study the DC and RF voltage spaces to obtain optimum ion-collection efficiency and mass resolution for the radicals studied.

Another factor that contributes to the size of the Si_xH_n radical signals is the transmission of the mass spectrometer, at the resolution required to fully separate the $Si_xH_n^+$ peaks. This has been evaluated by comparing the current entering a 2 mm aperture into the quadrupole region, versus that leaving this region (see Fig.2). A typical transmission in this mass 30 region is 10%. In the mass region of 56-62, corresponding to the disilane radicals Si_2H_n, this transmission has dropped to ~ 2 %, and for H and H_2 it is near 50%. Thus, we are most sensitive to H atoms, once H^+ is well resolved from H_2^+ and "zero mass" by switching the mass spectrometer frequency to 5 MHz.

6. Gas Handling System

The gas handling system includes a ~ 950 °C gas pyrolizer between the turbomolecular and final rough pump, to break down the silane gas into Si plus hydrogen gas that can be vented safely. Similarly, ultra-high vacuum, stainless steel valves control the inlet and outlet gas flows. The pyrolizer is placed between the rough pumps that evacuate the

chambers and another rough pump that prevents air from back streaming into the pyrolizer. This pyrolizes silane into surface-bonded Si and H_2 gas that can be safely vented. Similarly, ultra-high vacuum, stainless steel valves control the inlet and outlet gas flows.

The pyrolysis produces a dense, loose layer of Si-metal alloy flakes over a period of a year or two, and we must prevent small flakes from backstreaming from the pyrolyser into turbo molecular pump bearings when the system is brought up to air. For this reason the pyrolyser has been placed after two rough pumps that evacuate the three turbo pumps. But one must also prevent air backstreaming into the pyrolyser, so a third (small) rough pump evacuates it. Most rough pumps are not designed for vacuum integrity at the outlet side, so this required modifying the first two rough pumps to achieve an outlet vacuum. This extra effort is the disadvantage of this approach, but the advantage of this pyrolysis method is that it is reliable, inexpensive and effective; it is obvious if a rough pump is not working, and no silane fires or explosion problems have occurred in connection with its use for > 20 years. However, some turbo-pump bearing have failed due to the aforementioned flake problem, and this new design should overcome this problem. This new pyrolysis system is now completed and working, and the inlet gas-handling system has also been constructed, assembled and evacuated, and is connected to silane, hydrogen and argon gases.

The following photographs show the completed vacuum apparatus, that encompasses the discharge chamber, differential pumping chambers, mass spectrometer, three turbo pumps, three rough pumps, inlet control valves and the pyrolyser. The QMS is mounted inside the left flange in Fig.5, and the discharge chamber is to the right. Fig. 6 shows the pyrolyser and rough pumps in detail. The pyrolyser is a ~ 2′ long, 2′′ diameter stainless tube, with three smaller stainless tubes pressed inside to assure gas contact with a hot surfaces and to strengthen the outer tube, which weakens as it alloys with silicon. This is externally heated to 900-950 °C, by heaters enclosed in insulating alumina wool and then aluminum foil. The tube is water cooled at the ends to protect the vacuum flanges.

For measurements of discharges in silane/hydrogen gas mixtures, a much larger H_2 gas flow must be handled by the pumps. To achieve this, a Roots pump is added between the discharge-chamber turbo pump and the rough pump seen here.

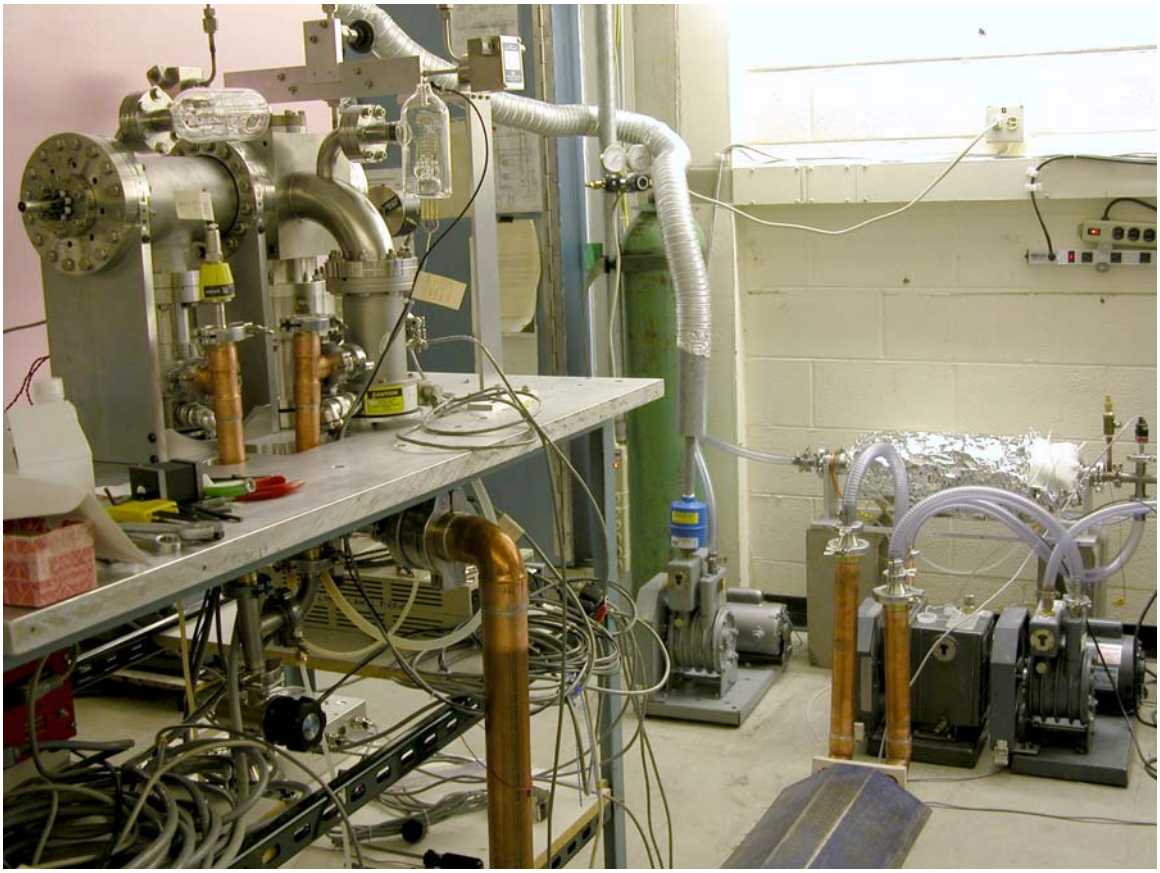

Fig.5. Vacuum apparatus, with the mass spectrometer flange at the upper left and the rough pumps and pyrolyser at the lower right. The hydrogen gas that exits the pyrolyser is vented out the top of the building through the flexible aluminum tube in the middle of the photograph.

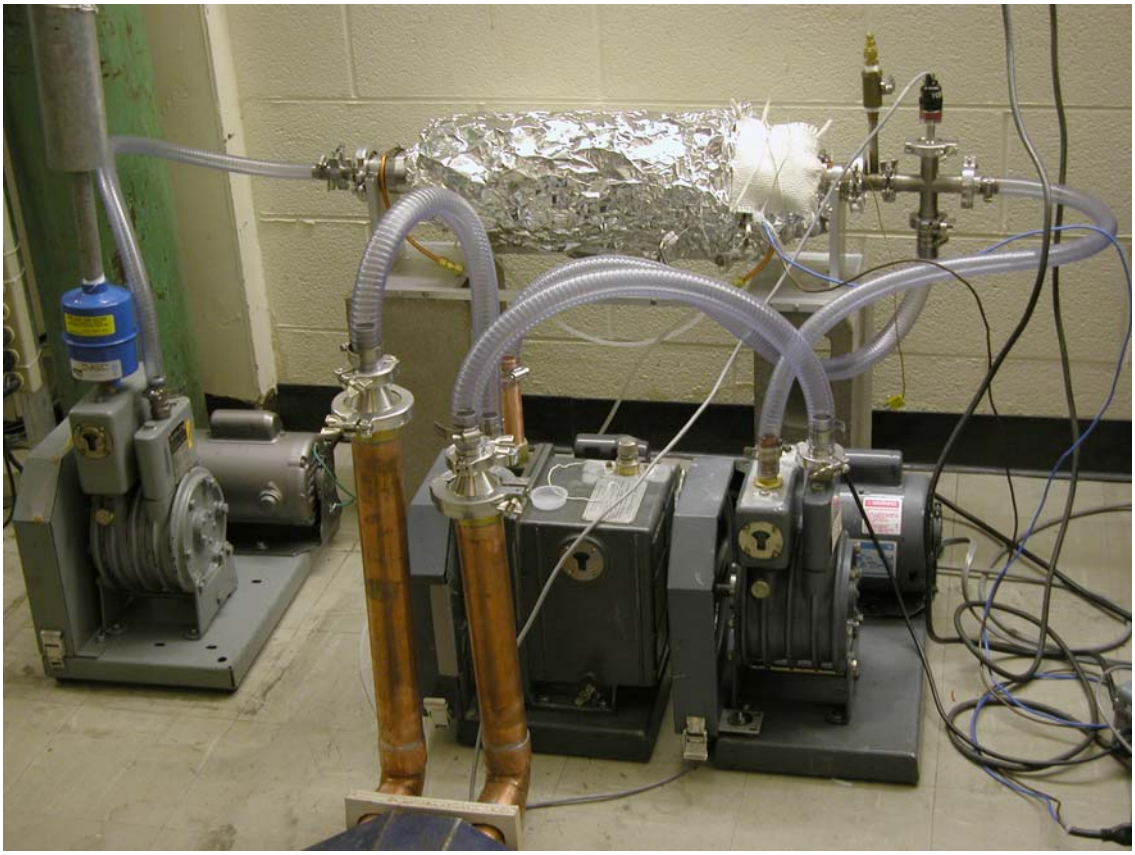

Fig.6. Photograph of the rough pumps and pyrolyser. The (larger) middle rough pump exhausts the discharge-chamber turbo, and the (smaller) right pump exhausts the differential-pumping and mass-spectrometer turbos. The outlet of the right pump must be vacuum tight, to avoid silane release into the atmosphere. This pump prevents hydrogen backstreaming into the mass spectrometer chamber, since turbo pumps have comparatively low compression ratios for hydrogen. The third rough pump, left, exhausts the pyrolyser, seen at the center top of the photo. This prevents air from entering the pyrolyser.

Results

1. Film Growth Rates

The power delivered to a RF discharge is typically only 10-20% of the power to the matching network, which is normally measured in device reactors. Thus, it appears best to compare "discharge power" conditions using film growth rates. We therefore measure film-growth rate (G) versus silane pressure, hydrogen pressure and discharge RF voltage, then measure the discharge radicals and ion versus these same parameters, effectively relating them to film deposition rate. A vacuum window and a small hole through the cathode allows film-thickness measurement using 780 nm laser reflection fringes in the a-Si:H film. Film thickness changes as small as ~0.01 nm can be measured, allowing also observations of the influence of starting transients and film surface changes following

changes in growth conditions. This does not provide the detailed film-surface information achievable with ellipsometry, but it is sensitive to film properties and readily shows any lack of reproducibility.

Most industrial and experimental reactors measure the ratio (R) of H_2 versus SiH_4 flows, the reactor chamber pressure (P_{Ch}). The RF voltage (V_{RF}) applied to the discharge is easy to measure, and is also monotonically related to the discharge power, so we measure G versus R, P_{Ch} and V_{RF} to relate our conditions to those of device makers. In essence, similar conditions exist in different reactors when the values of G, R and P_{Ch} are the same. There are actually several additional variables that these parameters do not provide. One is the silane depletion in the reactor. The actual R value of the gas mixture depends on this depletion, and can become much higher than the inlet H_2/SiH_4 flow ratio. Furthermore, disilane builds up in the chamber, and can be important. Sometimes it is possible to estimate this depletion from G, if the gas flows are well confined to the reactor volume. Another variable is the electrode gap; we utilize a 2 cm gap, which is in the middle of the range used for in many reactors. Two additional variables are the temperatures of the substrate (T_{Sub}) and the RF electrode (T_{RF}). While T_{Sub} is normally measured and reported, T_{Sub} -T_{RF} can also be important and is normally not known.

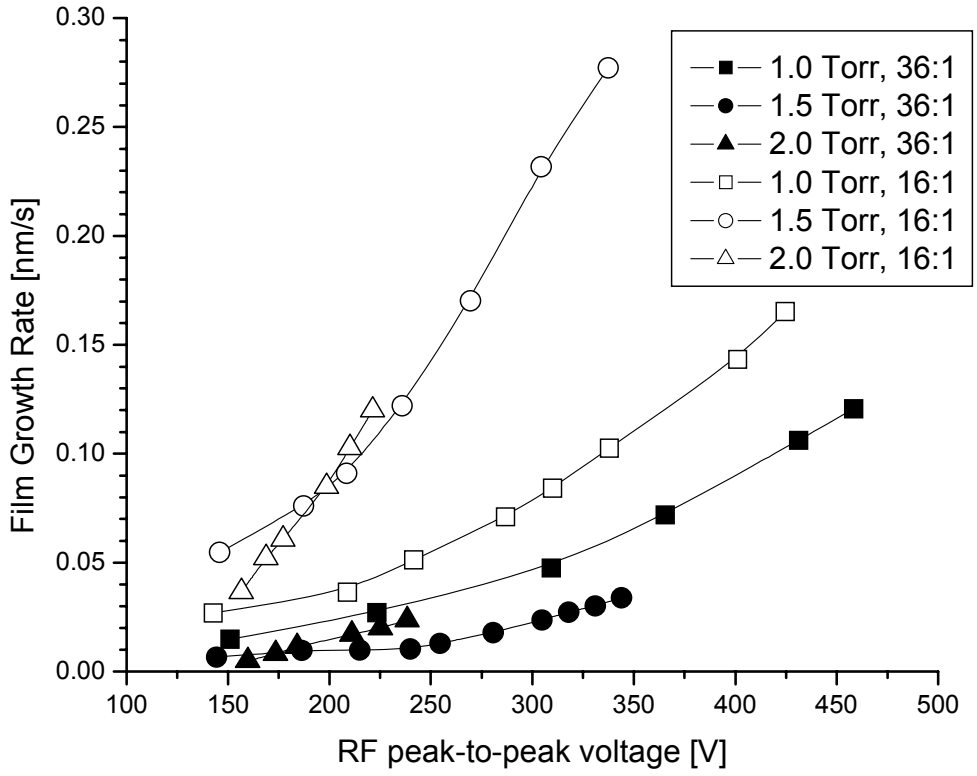

Fig.7. Film growth rate (G), versus V_{RF} and P_{Tot}, for R = 16 and 36.

The film-growth rate data, for a range of conditions, is shown in Figs. 7 and 8. These measurements were carried out with the entire discharge chamber at 300K. Primarily the vapor densities influence the discharge behavior, so for an isothermal chamber at the typical operating temperature of 500 K, the pressures should be multiplied by 5/3.

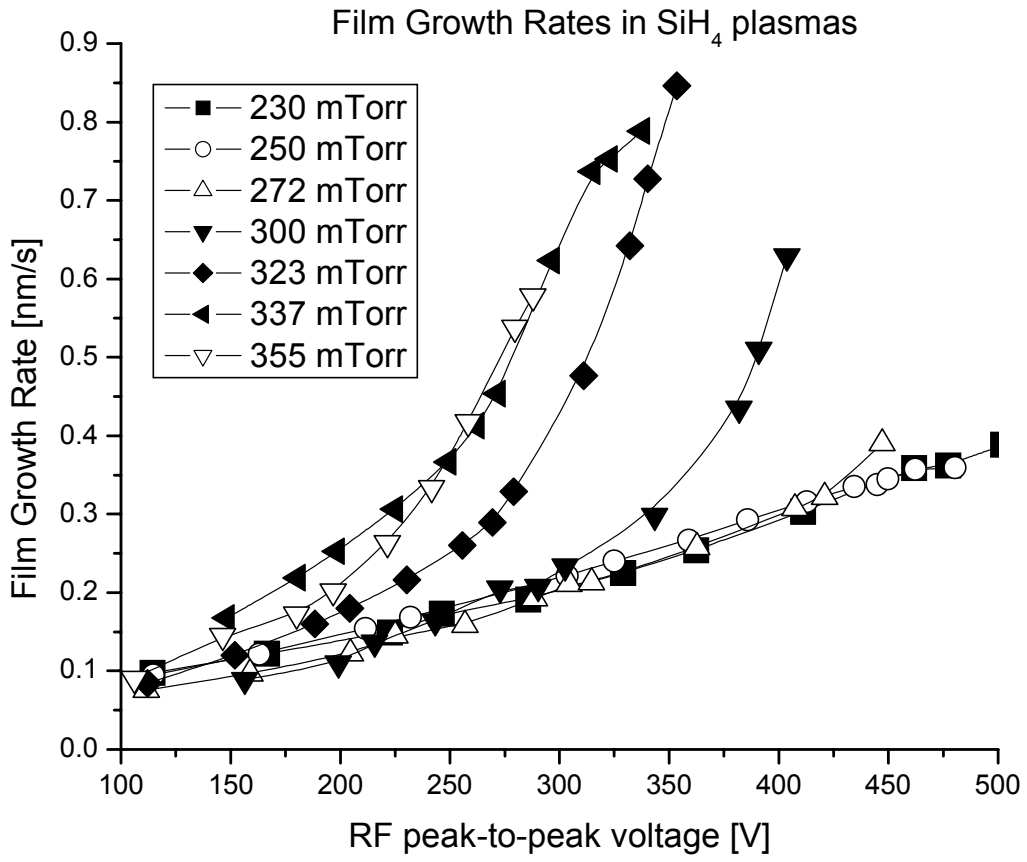

Fig.8. Film growth rate with pure silane inlet flow, versus pressure and V_{RF}. The silane depletion is 15% at 0.35 nm/s film growth rate.

Comparing Figs. 7 and 8, one can see that diluting the silane to R = 16 does not have a major influence on G, at least for P_{Tot} = 1.5 and 2.0 Torr. The silane pressure is ~0.1 Torr for these cases, which are "on the edge" of producing microcrystalline films. However, diluting further to R = 36 reduces G by a factor of 5-10. Here the hydrogen etching is seriously competing with silicon deposition, and microcrystalline films are being produced. This reduction in G can be partly compensated by increasing V_{RF}, but this is accompanied by an increase in ion bombardment energies.

2. Stable Gases

As silane is depleted in the discharge, the silicon atoms go into the a-Si:H film or higher silanes, primarily disilane (Si_2H_6). The disilane is a minor fraction of the gas, but it plays a major role in the plasma chemistry and an even larger role is silicon particle growth. We also have to know the disilane density in the discharge to calibrate the mass spectrometer measurements of Si_2H_n radicals that contribute to film growth. Thus, it is desirable to measure how much of the depleted silane yields disilane and higher silanes, versus film. This branching has been measured for pure silane discharges, also in this laboratory, but most device deposition is now done using hydrogen-diluted silane. We have therefore measured this branching for the type of silane/hydrogen mixtures now used in device production, and versus temperature. Our full results are available in the publication "Production of higher silanes in radio frequency SiH_4 and H_2-SiH_4 plasmas".[8]

This knowledge of the amount of stable gases disilane and trisilane that are produced in H_2-SiH_4 discharges has been used to calibrate the mass spectrometer signals from the discharge for these higher-silane species. However, the substrate temperature is 300 K, not the typical 500 K. The pressure is 0.3 Torr, of which 95% is SiH_4 and the remainder is H_2 from (~ 10%) decomposed SiH_4. The electrode gap is 2 cm and the film growth rate is near 0.1 nm/s.

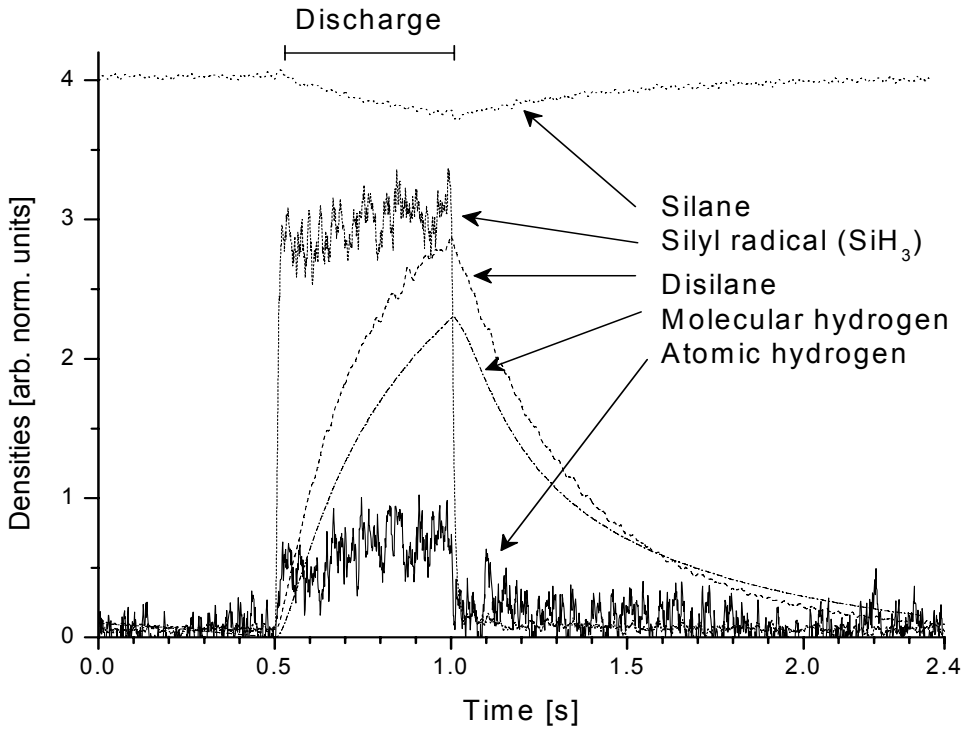

Fig. 9 Time dependence of densities during discharge. Signals are arbitrarily normalized to show on the same scale; backgrounds are subtracted. The electron energy is 25 eV for the stable gases, and different for the radicals as explained in the text. These signals are shown with arbitrary size: the data described above provides absolute scales for the H_2 and Si_2H_6 densities.

In order to avoid excessive particle production in the reactor and thus clogging the pumping orifices, the discharge is pulsed: typically turned on for 0.5 s, then off for 2 s. The gas flow then carries silicon particles out of the discharge region while there are small enough (<10 nm dia. [3]) to avoid clogging of the apertures and turbo pump. A second advantage of the discharge pulsing is that it can be used to verify the detection of radicals. These appear only during the discharge, whereas the densities of stable gases change slowly with discharge switching. The time dependence of the stable gas and radical densities, detected by the mass spectrometer during the pulsed discharge, is shown in Fig. 9. Note the rise and decay of stable species and step changes in radical and atomic hydrogen densities.

3. Radicals

In order to detect radicals, we measure the TIMS signals versus electron energy, using electron energy below the stable-gas, dissociative-ionization threshold. Two different electron currents are used for each electron energy, to allow subtraction of the signal from the discharge ions that leak through the deflector grids. The result of such a measurements for mass 31 (SiH_3^+) is shown in Fig. 10.

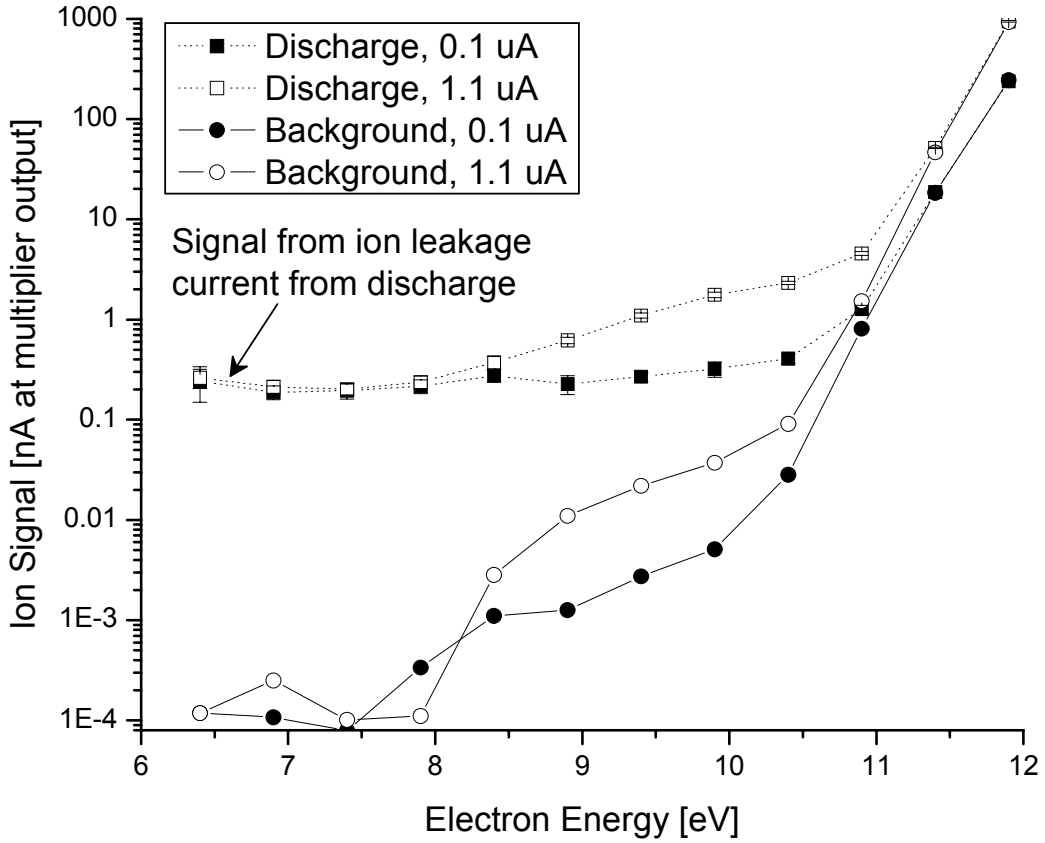

Fig. 10. SiH_3^+ signal versus electron energy below the SiH_4 dissociative ionization threshold. TIMS signals are averaged during and after the switched discharge.

Ions escaping from the discharge and leaking through the deflector grids yield the 0.2 nA signal at low E_{el}. This parasitic signal does not depend on the ionizer electron current or energy. (This leakage current is 10^{-5} of the ion current before applying voltage to the deflector grids.) One can also note that, due to finite electron temperature, we detect some signal from the dissociative ionization of silane even below its 12.3 eV threshold.
After the ion background is subtracted, the signals due to ionization by the electron beam (during and after the discharge) are obtained, as in Fig. 11. The radicals arriving from the discharge are clearly identified by their specific ionization threshold.

The electron energy scale and MS sensitivity for SiH_n radicals are calibrated with a threshold scan of $SiH_4 \rightarrow SiH_2^+$ from a known silane pressure in the discharge chamber (without discharge). After a minor correction for background silane gas in the ionizer region, versus only a molecular beam for the radicals, this provides a calibration of the radical density at the substrate. (We assume a similar cross section for direct ionization of all the SiH_n in the threshold-energy region where only one ion species occurs.) Measurements of disilane radicals (Si_2H_n, n = 0-5) have also been made. At the required mass resolution, the mass spectrometer is much less sensitive for these disilane radicals versus the SiH_n radicals. The mass spectrometer signals for the Si_2H_n radicals are calibrated in terms of density by comparing to direct near-threshold ionization of a known density of Si_2H_6 in the discharge region. This Si_2H_6 is actually produced by the SiH_4 discharge, with the amount known from our prior quantitative measurements of the discharge production and destruction of Si_2H_6.[8] The $Si_2H_2^+$ signal versus cathode voltage is shown in Fig. 12. The other Si_2H_n radical signals are considerably smaller than this Si_2H_2 signal, and will not be shown. The electron energy is typically 2.6 eV lower than the cathode voltage, mostly due to contact potential differences between the Ba cathode surface and the carbon ionization-chamber surfaces. Thus, the "discharge on" signal in Fig.12 is consistent with an 8.0 eV threshold, about as expected for $Si_2H_2 \rightarrow Si_2H_2^+$.
We observe that, for a typical 0.3 Torr pure silane discharge operated at 200 V_{pp} RF voltage, which yields a deposition rate of 0.1 nm/s, the density of SiH_3 is 2.2×10^{11} cm^{-3}, which is 2.2×10^{-5} that of SiH_4. Similar measurements with atomic hydrogen versus H_2 yield a density of H at the substrate that is ~ 4 % of SiH_3 density under these conditions. However, the background-gas correction is much larger and more uncertain for H_2, so this result is uncertain by a factor of 2. The densities of the other SiH_n radicals are quite small; the measured density of SiH is 5% of the SiH_3 density, while we have set upper limits of 0.1 and 1 % of SiH_3 for the Si and SiH_2 radicals. The radical densities observed from a 0.3 Torr, 100 C, 200 V pure silane discharge are shown in Fig. 13.

Only the radicals SiH_3 and Si_2H_2 have been observed from R= 16 and 36 silane-hydrogen discharges. This data, and upper limits on the other species is shown in Figs. 14 and 15.

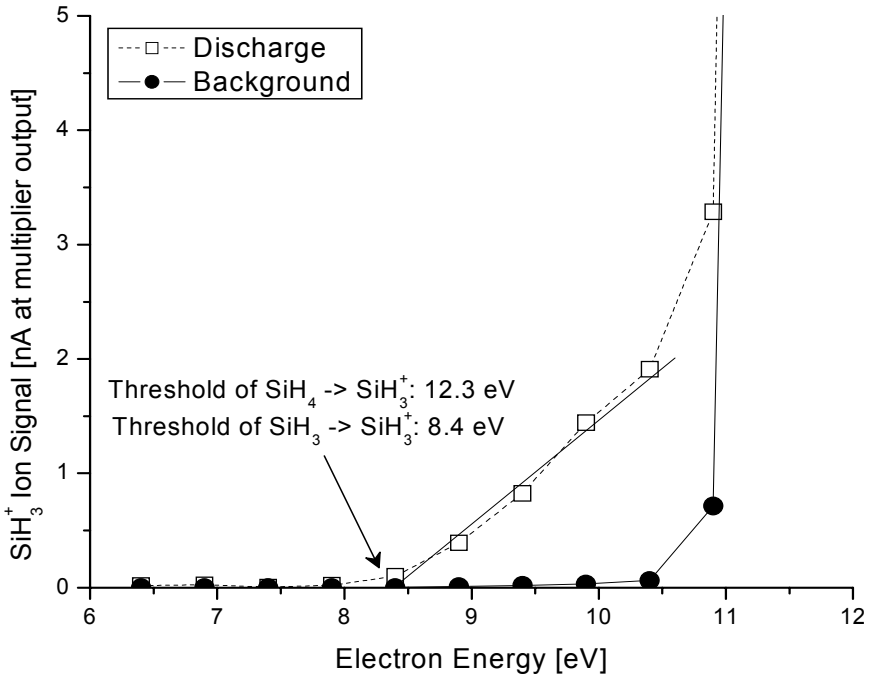

Fig. 11. Detection of SiH_3 radicals: energy scan below the $SiH_4 \rightarrow SiH_3^+$ threshold. The signals at two different electron currents are subtracted, thus eliminating the signal from ion leakage.

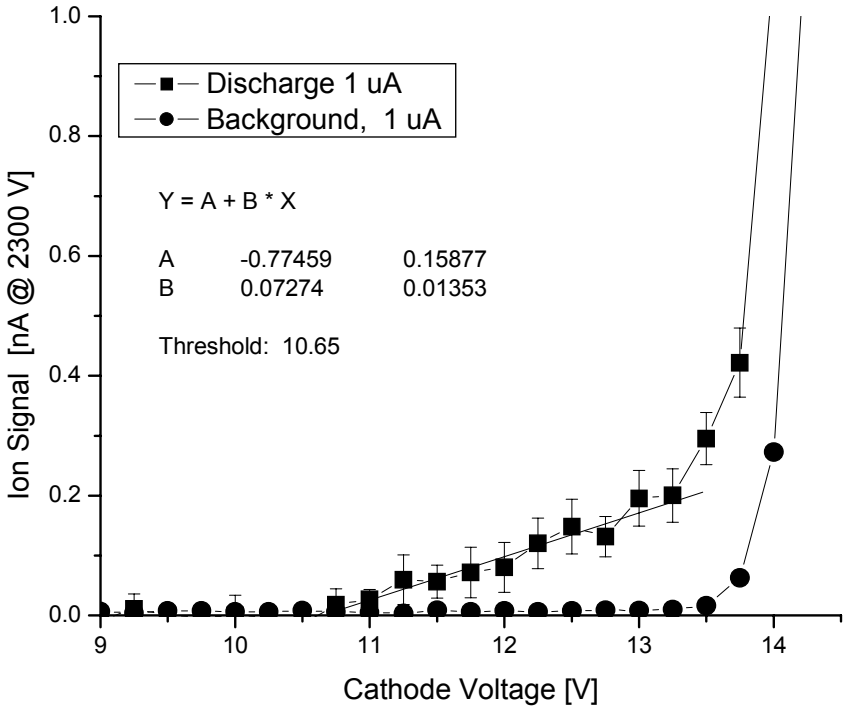

Fig. 12. Mass 58 signal versus electron-beam cathode voltage, with and without discharge. The ion background has already been subtracted from both signals.

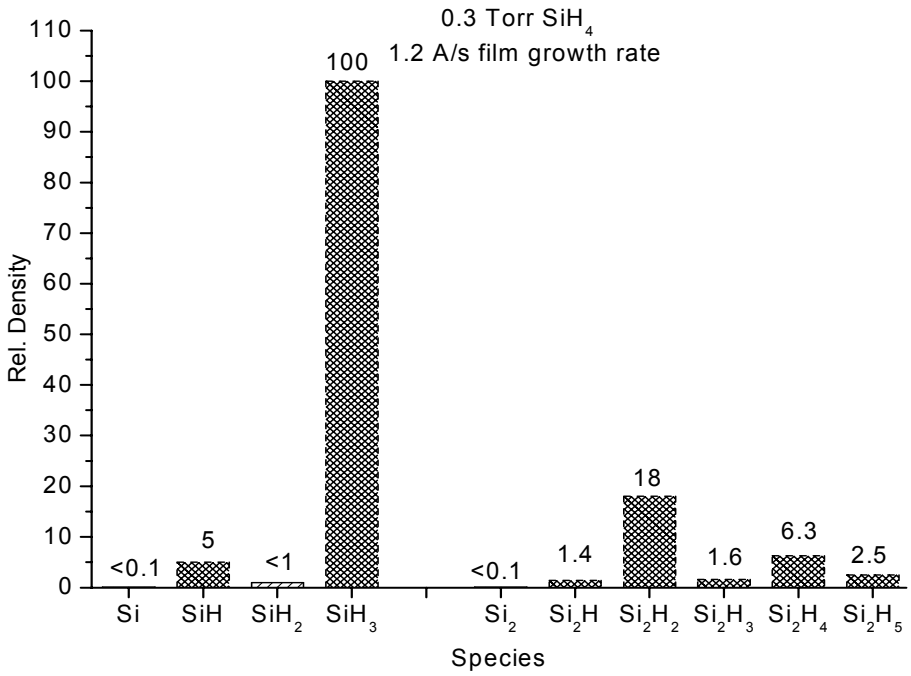

Fig. 13. Radical densities at the substrate of a 0.3 Torr, 100 C, 200 V, pure-silane discharge. The Si, SiH_2 and Si_2 densities are upper limits.

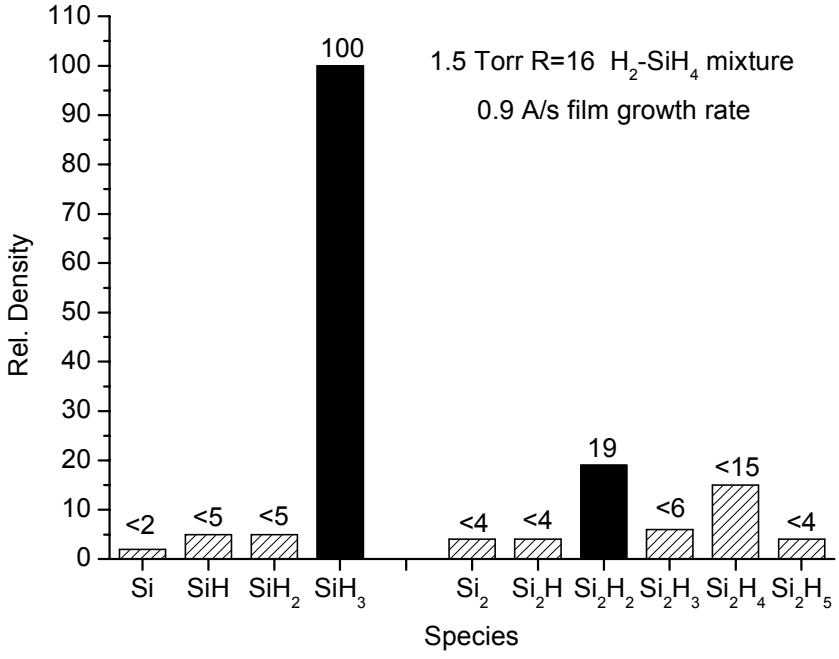

Fig. 14. Radical densities at the substrate of a 100 C, R= 16 silane-hydrogen discharge, with V_{RF} = 200 V (p-p).

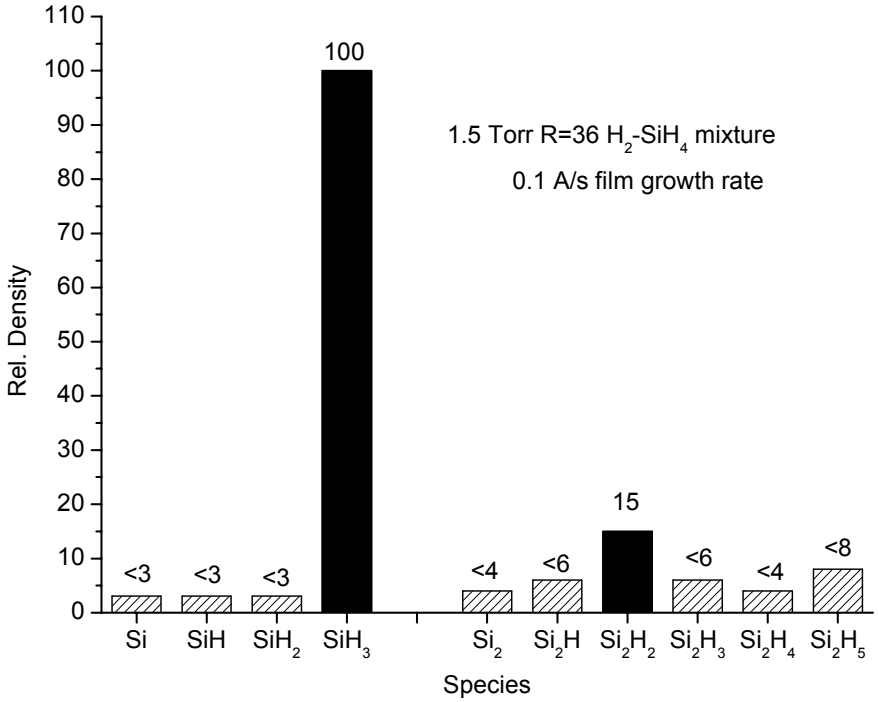

Fig. 15. Radical densities at the substrate of a 100 C, R= 36 silane-hydrogen discharge, with V_{RF} = 200 V (p-p).

The flux (F_{xm}) of Si atoms carried by a radical to the substrate is the most important indicator of the contribution of this radical (Si_xH_m) to film growth. Our TIMS signals are proportional to the portion (n_{xm}) of the radical density at the substrate that is moving toward the surface (where the small aperture allows some to pass through to the ionizer). From the kinetic-theory boundary condition, the radical flux that reacts with the substrate is $FR_{xm} = n_{xm}v_x\beta_{xm}/2$, where v_x is the mean radical velocity and β_{xm} is the reaction probability (per collision) on the substrate; actually the growing silicon-film surface. A fraction γ_{xm}/β_{xm} of this flux yields deposition of one Si-atom, or $F_{xm} = n_{xm}v_x\gamma_{xm}/2$, where x Si atoms are carried by each radical. Thus, comparing Si_2H_2 to SiH_3, $F_{22}/F_{13} = (n_{22}/n_{13})(v_2/v_1)(\gamma_{22}/\gamma_{13}) = (0.2)(0.7)(\gamma_{22}/0.09) \cong 1.6\ \gamma_{22}$, using a measured $\gamma_{13} = 0.09$.[7] If Si_2H_2 reacted with high probability, incorporating 2 Si atoms, this would yield $\gamma_{22} = 2$ and a Si_2H_2 contribution to film growth that exceeds that of SiH_3 by a factor of 3. But a calculation of F_{13}, using the above measured n_{13} and including several experimental uncertainties, yields 0.066±0.03 nm/s film growth rate (G) from SiH_3, compared to a measured G = 0.1±0.02 nm/s. These numbers agree within their uncertainties, and do not allow for a Si_2H_2 contribution that greatly exceeds that of SiH_3. Thus, we conclude that $\gamma_{22} << 1$; apparently there is a relatively stable form of Si_2H_2, similar to acetylene as the equivalent hydrocarbon, which has a small surface reactivity.

The reaction probabilities of the Si, SiH and SiH_2 radicals on a-Si:H are not known, but can be reasonably estimated as 50% for these very reactive radicals. Thus, in terms of reacting flux (F) to the film: $F(SiH_3) = 30$, $F(SiH_2) < 2$, $F(SiH) < 2$, and $F(Si) < 1$. It is

clear that, as expected, SiH_3 produces most of the film growth. However, these numbers allow for a significant fraction from the other SiH_n radicals, H reactions may be important, and the reactive flux of Si_2H_2 is not known. Thus, the radical mixture and film-growth might have significant dependence on the discharge parameters. Consequently, we are refining these preliminary analyses to provide better limits on the other radicals, particularly SiH_2 and the other Si_2H_n. We are also considering possible measurements that might yield the very important β_{xm} and γ_{xm} factors, to more accurately relate the surface density of each radical to its contribution to film growth. These are difficult to measure and very dependent on the surface structure. For example, a H reaction probability of 0.1 on a-Si:H has been measured on a-Si:H with a thermal technique,[9] a value of 0.4 has been measured on μc-Si (incorrectly identified as a-Si:H in the manuscript) using TIMS,[10] and 0.8 has been measured on sputtered Si using H^* emission to identify H.[11]

4. Discharge Ions

Ion flux to the substrate is known to be typically a few percent of the radical flux, so ions do not have much effect on the film growth rate. However, energetic ions containing Si can alter the structure of deep surface layers, below the region where film structure and electronic properties are largely frozen in. H_n^+ ions are not expected to penetrate below the top surface layers, nor do they have enough mass to directly alter structure in these layers. However, they can etch and rearrange Si-Si bonding in the surface layers, and they may be important in the amorphous to crystalline transition. It is therefore of interest to establish both the impacting ion energies and species. The ion energies were studied in reference 12, and here we measure the species. This is done by grounding the ion-deflection screens, thereby allowing ions to pass through to the mass spectrometer. This detects ions that are directed towards the substrate at or close to the surface normal, but as the more energetic ions have such motion this is of primary interest. The ion species H_n^+, SiH_n^+, $Si_2H_n^+$, and $Si_3H_n^+$ have been measured. H_3^+ totally dominates the H_n^+ ions, so a figure is not provided for these ions. Data that shows the n dependence of the silane ions for R = 0, 20 and 40 discharges is shown in Figs.16-18. The relative contributions of the $H_3^+$and $Si_xH_y^+$ ions (summed over y) in H_2/SiH_4 mixtures are shown in Figure 19, versus the silane to hydrogen ratio. Essentially no H_n^+ ions are observed from pure silane discharges, so only the measured fractions of $Si_xH_n^+$ (summed over n) are plotted in Figure 20. This data is from room temperature discharges excited by 200-270V RF peak voltage, for pressures of 0.3-0.5 Torr, and it is plotted versus RF voltage divided by pressure. Short, pulsed discharges are used for all of this data, so the pressures of hydrogen and silane vapor are not significantly modified by the discharge.

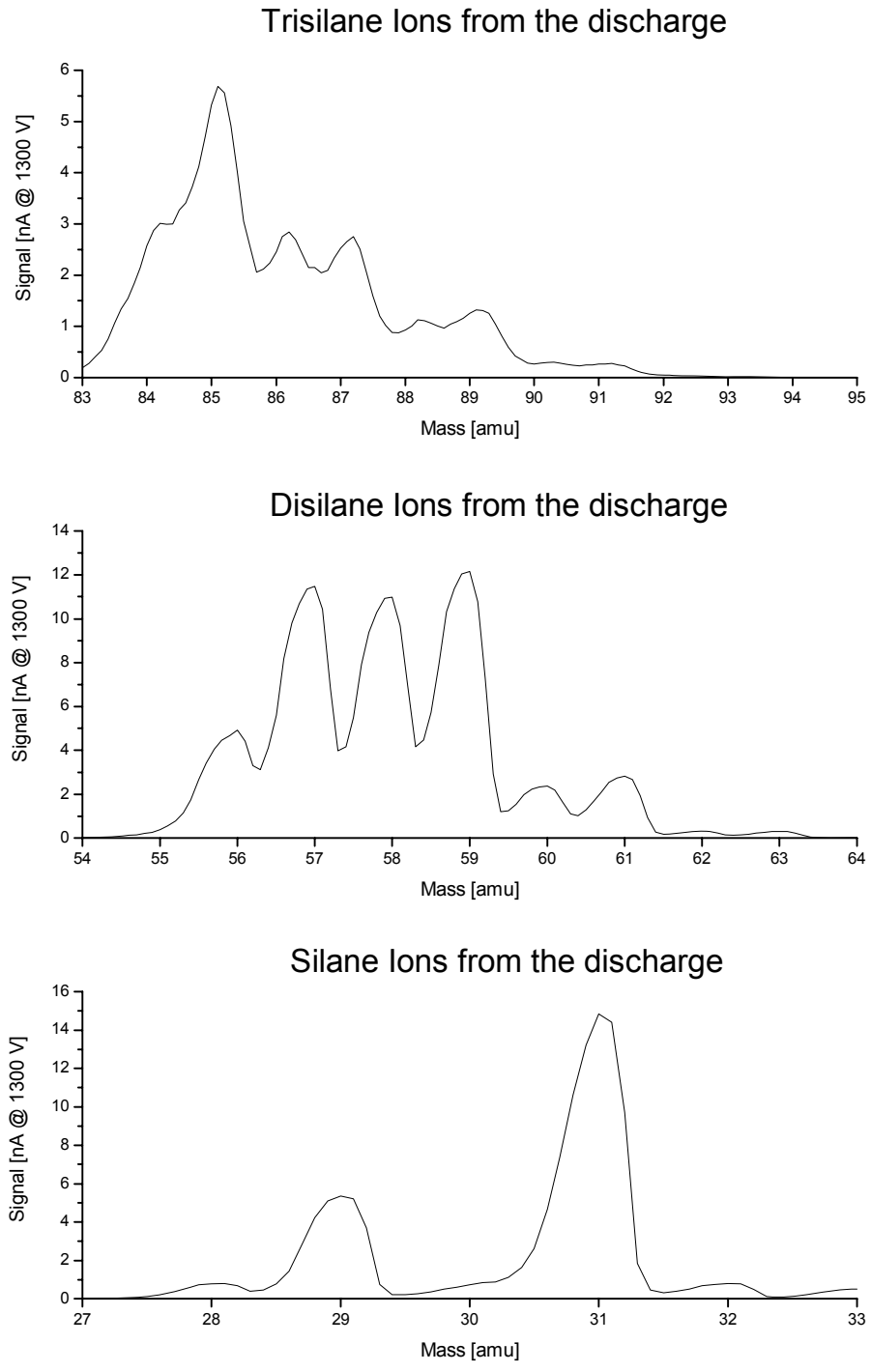

Fig. 16. Ions from a 0.3 Torr, 200 V, 100 C pure-silane discharge.

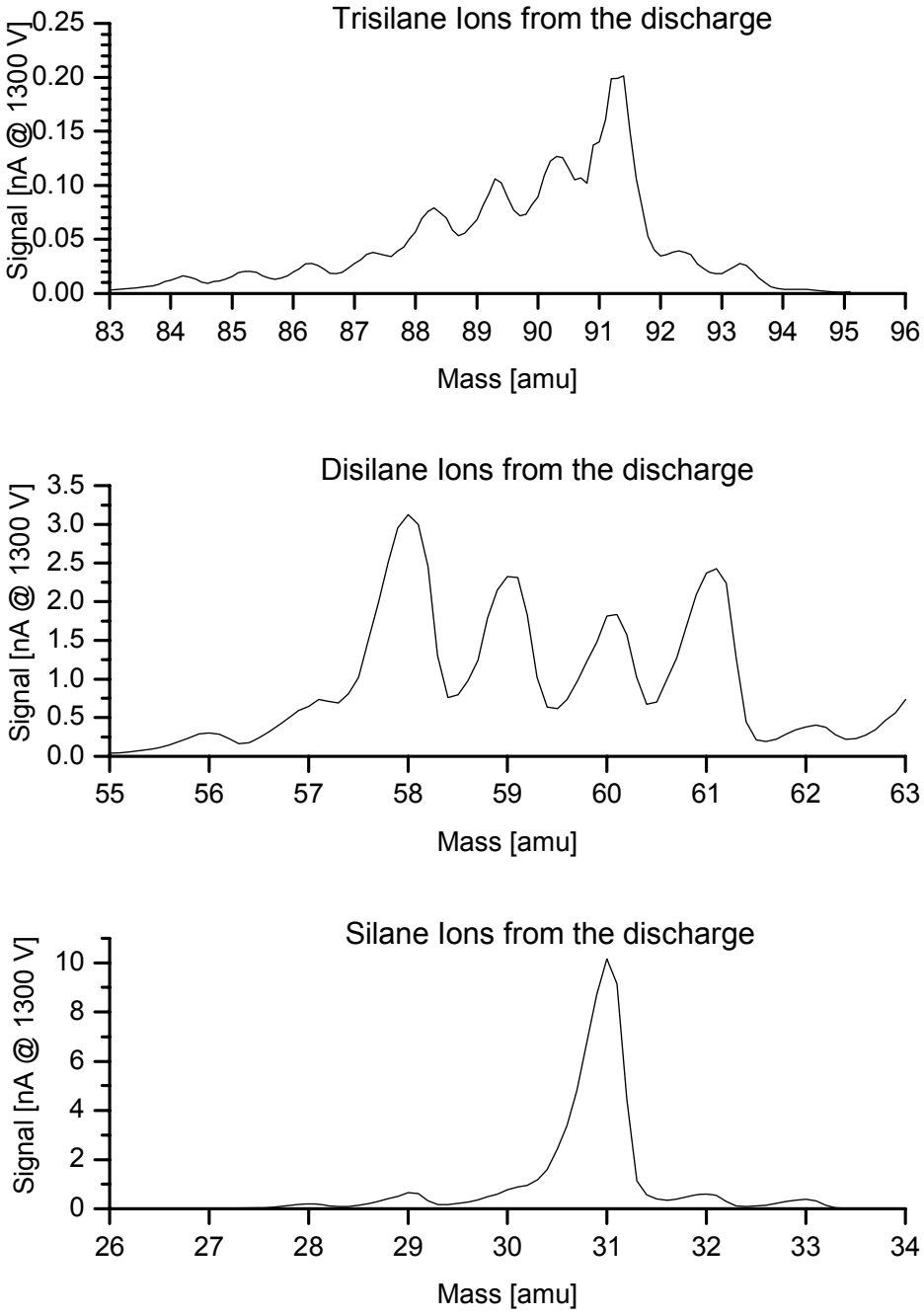

Fig. 17. Ions from a 1.5 Torr, 200 V, R = 20 silane-hydrogen discharge.

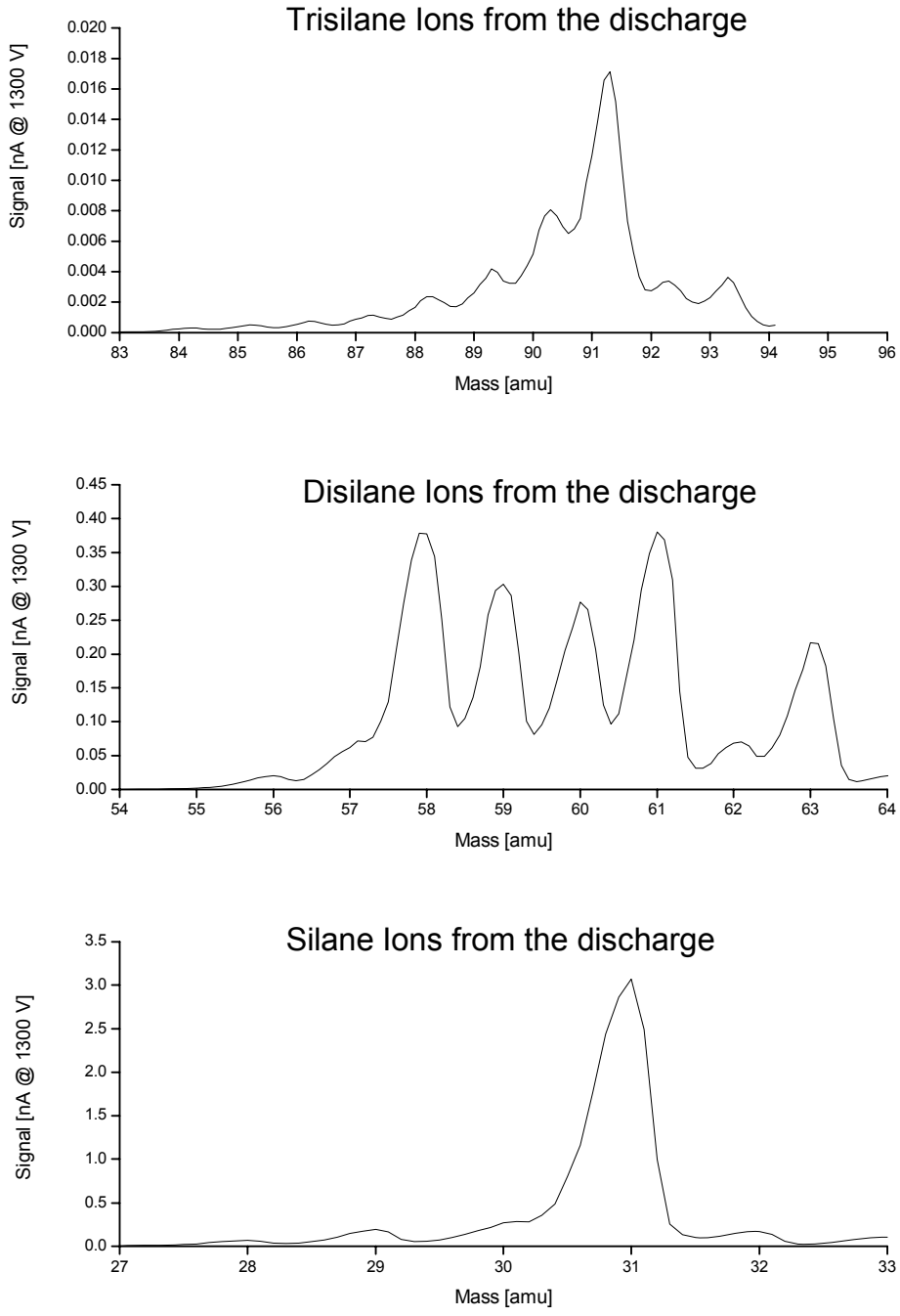

Fig. 18. Ions from a 1.5 Torr, 200 V, R = 40 silane-hydrogen discharge.

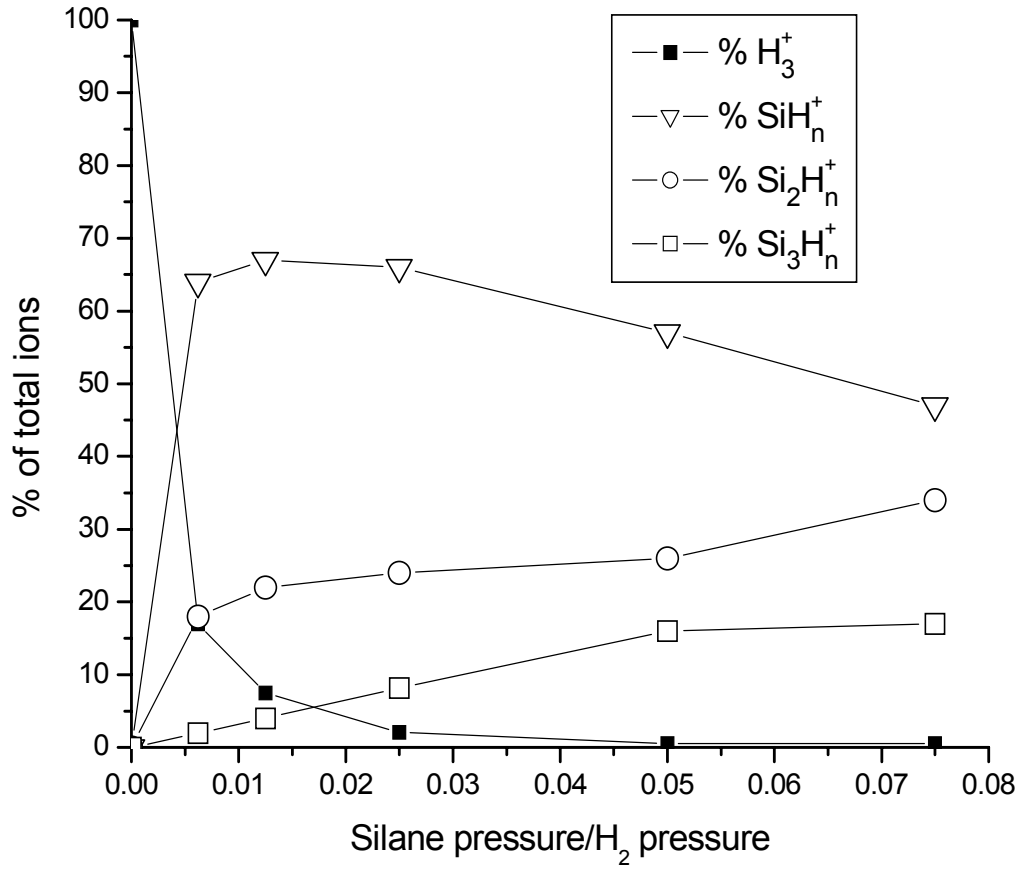

Fig. 19. Types of discharge ions at the substrate of a silane/hydrogen RF discharge, versus the pressure (inlet flow) ratio of silane to hydrogen. (This ratio is 1/R.) The conditions are 230 V (peak) RF voltage and a total pressure of 1 Torr at 300 K. The $Si_xH_n^+$ ions have been summed over n.

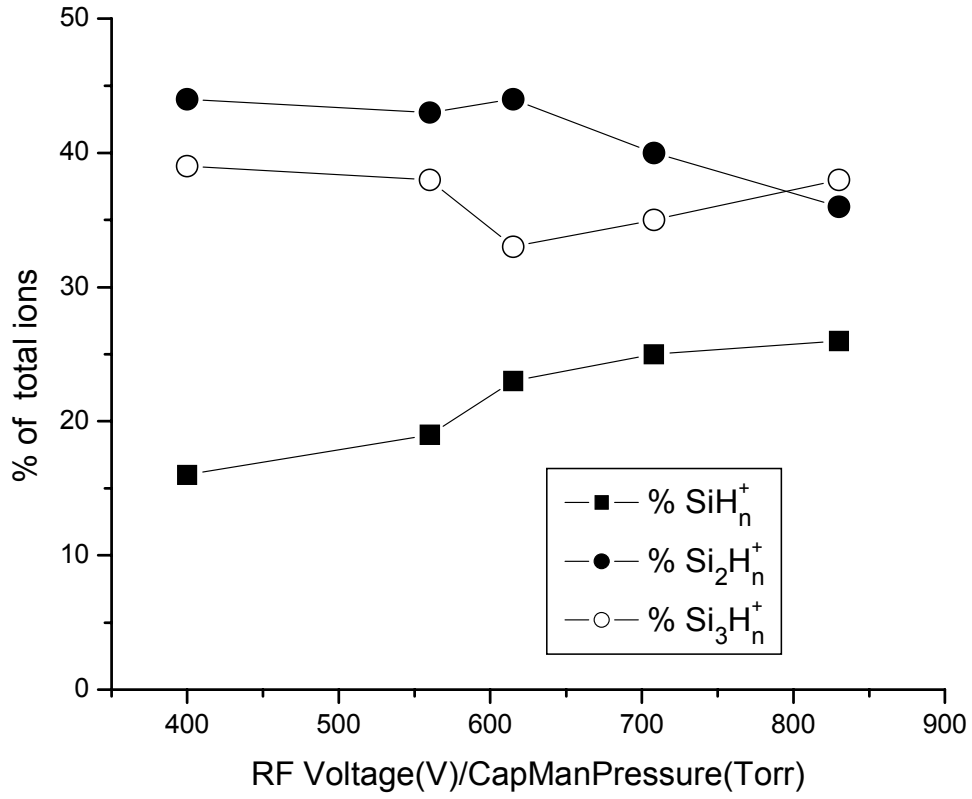

Fig. 20. Types of ions at the substrate of an RF discharge in pure silane, versus peak RF voltage (V) divided by pressure (Torr). The $Si_xH_y^+$ have been summed over y.

These observations yield several interesting results that are important to understanding how ion bombardment of the substrate can influence device properties. (1) The flux of H_n^+ ions is negligible under all conditions where devices are grown (R < 100 or SiH_4/H_2 > 0.01). Thus, these ions are not a cause of the changing film properties, from amorphous to micro-crystalline, versus hydrogen dilution (R value). (2) The number of Si atoms in the bombarding ions (x in $Si_xH_y^+$) is only weakly dependent on hydrogen dilution (R) for R <30, but the large-x ions contribute much less for R > 30 and in pure silane. As even larger x values than the ones studied here (up to x = 3) doubtless also contribute to the ion flux, this is a significant change. The heavier ions are expected to have much lower impact energies per Si atom, so they could remain together and introduce a comparatively large Si cluster at the growing surface. (3) The H content (y in $Si_xH_y^+$) is almost constant versus R in the hydrogen-diluted vapor, but it is much smaller in pure silane. We suspect that this results from a much smaller center-of-mass ion-molecule collision energy in ion-H_2 collisions, compared to ion-SiH_4 collisions. The influence of this on film properties is not known or easily conjectured.

Conclusions

The present observations of SiH_n and Si_2H_n radical densities at a-Si:H and μc-Si substrate surfaces indicate that SiH_3 is the most abundant radical, but significant amounts of Si_2H_2 also occur. Other smaller density components such as SiH and Si_2H_4 occur for a pure silane discharge, but are below detection limits for the R = 16 and 36 discharges. Since SiH_3 is relatively inefficient at depositing Si into the film, these other radicals could provide a significant (> 10%) contribution to film growth, and thereby also to device properties. The radical density that should vary the most with R (hydrogen dilution) is, of course, the H atom. Our current data is ambiguous regarding H atom densities, so we do not report these preliminary results here. There is a strong indication that H densities at the substrate vary with surface condition as well as with R, but this still has to be verified.

The other radicals that arrives at the growing film surface are the positive ions. Although their flux is a small fraction of the radical flux, due to their high energies and clustering they can be important. We measure here the ion spectra, but not the energy with which they bombard the surface. We find that the mixture of $Si_xH_y^+$ radicals is fairly similar for R = 15-100 discharges, although the heavier (larger x) species are of decreasing importance as R increases. The ions contain fewer H (smaller y), and larger x values are more important, in the pure silane, R=0 case. The only significant H_n^+ ion is H_3^+, and this occurs in unimportant quantities in all cases used for device production (R < 100). Since ions typically induce 1-5% of film growth, these changes in $Si_xH_y^+$ mixtures versus R could be significant for device properties. However, it has also been shown that the average ion bombardment energy decreases with hydrogen dilution,[12] and this may be the most important dependence on R.

References

1) "Radical species in argon-silane discharges," R. Robertson, D. Hils, H. Chatham and A. Gallagher, Appl. Phys. Lett. 43 (1983) 544-546.

2) "Mono- and disilicon radicals in silane and silane-argon dc discharges," R. Robertson and A. Gallagher, J. Appl. Phys. 59 (1986) 3402-3411.

3) "Study on the absolute density and translational temperature of Si atoms in very high frequency capacitively coupled SiH_4 plasma with Ar, N_2, and H_2 dilution gases" T. Ohta, M. Hori, T. Ishida, T. Goto, and S. Kawakami, Japanese Journal of Applied Physics 43 (2004) 6405-6412.

4) "Laser-induced-fluorescence study of the SiH_2 density in RF SiH_4 plasmas with Xe, Ar, He, and H_2 dilution gases" A. Kono, N. Koike, H. Nomura, and T. Goto, Japanese Journal of Applied Physics 34 (1995) 307-311.

5) "Measurement of absolute densities of Si, SiH and SiH_3 in electron cyclotron resonance SiH_4/H_2 plasma" Y. Yamamoto, H. Nomura, T. Tanaka, M. Hiramatsu, M. Hori, and T. Goto, Japanese Journal of Applied Physics 33 (1994) 4320-4324.

6) “Mass spectrometry detection of radicals in SiH_4-CH_4-H_2 glow discharge plasmas” P. Kae-Nune, P. J. Perrin, J. Guillon, and J. Jolly, Plasma Sources, Science and Technology 4 (1995) 250-9.

7) “Surface reaction probabilities and kinetics of H, SiH_3, Si_2H_5, CH_3 , and C_2H_5 during deposition of a-Si:H and a-C:H from H_2, SiH_4, and CH_4 discharges” J. Perrin, J. M. Shiratani, P. Kae-Nune, H. Videlot, J. Jolly, and J. Guillon, J. Journal of Vacuum Science & Technology A 16 (1998) 278-89

8) “Production of higher silanes in radio frequency SiH_4 and H_2-SiH_4 plasmas” P. Horvath, K. Rozsa, and A. Gallagher, J. Appl. Phys. 96, (2004) 7660.

9) “Measurement of the concentration of hydrogen radicals and their recombination probability on a-Si:H”, > Tsuji, T. Akiyama and H. Komiyama, J. Non. Cryst. Solids 198-200 (1996) 1034-7.

10) “Surface recombination probabilities of H on stainless steel, a-Si:H and oxidized silicon determined by threshold ionization mass spectrometry in H_2 RF discharges”, P. Kae-Nune, J. Perrin, J. Jolly, and J. Guilllon, Surf. Sci. Lett. 360 (1996)

11) “Study of the volume and surface processes in low pressure radio frequency plasma reactors by pulsed excitation methods. I. Hydrogen-argon plasma” A. Bouchoule and P. Ranson, J. Vac. Sci. Technol. A9 (1991) 317.

12) “Analysis of plasma properties an deposition of amorphous silicon alloy solar cells using very high frequency glow discharge” B. Yan, J. Yang, S. Guha, and A. Gallagher, Mat. Res. Soc. Symp. Proc. 557 (1999) 115.

REPORT DOCUMENTATION PAGE

Form Approved
OMB No. 0704-0188

PLEASE DO NOT RETURN YOUR FORM TO THE ABOVE ORGANIZATION.

1. REPORT DATE *(DD-MM-YYYY)*	2. REPORT TYPE	3. DATES COVERED *(From - To)*
June 2006	Subcontract Report	1 June 2002 – 31 May 2005

4. TITLE AND SUBTITLE
Measurement of Depositing and Bombarding Species Involved in the Plasma Production of Amorphous Silicon and Silicon/Germanium Solar Cells: Final Technical Report, 1 June 2002–31 May 2005

5a. CONTRACT NUMBER
DE-AC36-99-GO10337

5b. GRANT NUMBER

5c. PROGRAM ELEMENT NUMBER

6. AUTHOR(S)
A. Gallagher, K. Rozsa, P. Horvath, and D. Kujundcik

5d. PROJECT NUMBER
NREL/SR-520-40056

5e. TASK NUMBER
PVB65101

5f. WORK UNIT NUMBER

7. PERFORMING ORGANIZATION NAME(S) AND ADDRESS(ES)
National Institute of Standards and Technology (NIST)
Boulder, Colorado

8. PERFORMING ORGANIZATION REPORT NUMBER
DE-AC36-02GO10244
(DOE-GO)

9. SPONSORING/MONITORING AGENCY NAME(S) AND ADDRESS(ES)
National Renewable Energy Laboratory
1617 Cole Blvd.
Golden, CO 80401-3393

10. SPONSOR/MONITOR'S ACRONYM(S)
NREL

11. SPONSORING/MONITORING AGENCY REPORT NUMBER
NREL/SR-520-40056

12. DISTRIBUTION AVAILABILITY STATEMENT
National Technical Information Service
U.S. Department of Commerce
5285 Port Royal Road
Springfield, VA 22161

13. SUPPLEMENTARY NOTES
NREL Technical Monitor: Bolko von Roedern

14. ABSTRACT *(Maximum **200 Words**):* The objective of this study is to measure the molecular species that lead to the growth of hydrogenated amorphous silicon (a-Si:H) and microcrystalline silicon (μc-Si) photovoltaic (PV) devices from RF discharges. Neutral radicals produce most of the film growth during this PV-device production, and, by implication, radicals primarily determine the device structure and electrical characteristics. The most important feature of the present experiment is thus the measurement of neutral-radical fluxes to the substrate. Additional depositing species that can influence film properties are positive ions and silicon-based particles produced by the discharge; we also measure these positive-ion species here. Some studies have already measured some of these radical and positive-ion species in silane and silane/argon discharges, but not for discharge conditions similar to those used to produce most photovoltaic devices. Our objective is to measure all of these species for conditions typically used for device production. In particular, we have studied 13.6 MHz-excited discharges in pure silane and silane/hydrogen vapors.

15. SUBJECT TERMS
PV; thin film; solar cells; amorphous silicon; microcrystalline silicon; plasma; germanium;

16. SECURITY CLASSIFICATION OF:			17. LIMITATION OF ABSTRACT	18. NUMBER OF PAGES	19a. NAME OF RESPONSIBLE PERSON
a. REPORT	b. ABSTRACT	c. THIS PAGE			19b. TELEPONE NUMBER (*Include area code)*
Unclassified	Unclassified	Unclassified	UL		